34th Annual International Conference of the IEEE EMBS
San Diego, California USA, 28 August - 1 September, 2012

Nanotopography Effects on Astrocyte Attachment to Nanoporous Gold Surfaces*

Ozge Kurtulus and Erkin Seker, *Member, IEEE*

***Abstract*—Nanoporous gold, synthesized by a self-assembly process, is a new biomaterial with desirable attributes, including tunable nanotopography, drug delivery potential, electrical conductivity, and compatibility with conventional microfabrication techniques. This study reports on the effect of nanotopography in guiding cellular attachment on nanoporous gold surfaces. While the changes in topography do not affect adherent cell density, average cell area displays a non-monotonic dependence on nanotopography.**

I. Introduction

Nanotechnology has had a significant impact on the field of medical research [1, 2], where applications include targeted delivery schemes with nanoparticles [3], nanostructured surfaces for improved biosensor performance [4], drug delivery from porous materials [5], and nanostructured surfaces to guide physiological response [6, 7]. One such emerging material is nanoporous gold (np-Au), which is typically produced by selective dissolution of silver from a silver-rich gold alloy, by a process known as *dealloying* [8]. The resultant material, with an open pore structure (illustrated in Fig. 1 and Fig. 2), exhibits desirable attributes for multifunctional coatings, including large area-to-volume ratio, high electrical conductivity, tunable nanoporosity, and well-defined thiol-based surface modification capabilities. These properties sparked interest in the scientific community to employ np-Au in fuel cell applications [9], fundamental studies of structure-property relationships [10], and biosensor applications [11]. We have previously demonstrated np-Au's potential for biomedical applications, where np-Au coatings on multiple electrode arrays enhanced signal-to-noise ratio in neural electrophysiological recordings [12]. Along with the ability to monitor physiological activity, it is also desirable to modulate it. One way to achieve this is by delivering drugs using nanoporous materials, where the pores act as drug reservoirs and nano-channels act as nozzles for controlling the release rate [13, 14]. Another approach is to modify nanotopography to modulate cellular response, such as adhesion strength and proliferation [6, 7]. The objective of this paper is to employ the latter approach and examine the relation between nanotopography of np-Au surfaces and cellular response, which are essential for engineering biomedical device coatings with minimal biofouling and maximal integration with cells of interest.

*Research supported by University of California, Davis – College of Engineering start-up funds.

E. Seker is with Department of Electrical and Computer Engineering at the University of California, Davis, CA 95616 USA (corresponding author; phone: 530-752-7300; e-mail: eseker@ucdavis.edu).

O. Kurtulus is with Department of Chemical Engineering and Materials Science at the University of California, Davis, CA 95616 USA (e-mail: okurtulus@ucdavis.edu).

II. Materials and Methods

A. Sample Preparation and Characterization

In order to evaluate the effect of nanotopography on cellular attachment, we created gold patterns with varying surface topographies. All films were deposited with a direct-current sputtering system (AJA Sputtering Instrument) through a 250 μm-thick silicone stencil mask with 5 mm-diameter holes. The gold spots were created by sequentially depositing 15 nm-thick chrome and 200 nm-thick gold layers. Np-Au is produced by selectively dissolving silver from a gold-silver alloy in a nitric acid (65%) bath at 50°C for 15 minutes. The precursor gold-silver alloy was created by depositing 15 nm-thick chrome, 50 nm-thick gold seed layer, and 300 nm-thick gold-silver alloy. The elemental composition of the alloy was determined to be $Au_{0.3}Ag_{0.7}$ (atomic %) with an energy dispersive spectrometer (Oxford Instruments) attached to a scanning electron microscope (Zeiss Ultra 55). Following the acid etch, the samples were rinsed and stored in deionized (DI) water for a week while replacing the water every two days. Different nanotopographies were obtained by thermally-treating a group of np-Au samples, where heat exposure leads to pore coarsening [15]. The treatment was performed in a rapid thermal annealer (Modular Process Technology) at 250°C, 350°C, and 450°C for 10 minutes. The coatings were imaged with the scanning electron microscope (SEM) exclusively using the secondary electron (SE) detector to maximize the acquisition of topographical information. The micrographs were analyzed with ImageJ image processing software to extract *percent void coverage* (total projection area of voids in an image divided by the image area) and *average void area*. Voids were defined as darker regions in each gray-scale image determined by an automatic thresholding algorithm [16].

B. Cell Culture and Quantification of Cellular Attachment

Cell culture media consisted of DMEM Advanced (Invitrogen) basal medium, 1X GlutaMAX (Invitrogen), 10% heat-inactivated fetal bovine serum (Sigma), and 0.2% Geneticin antibiotic (Invitrogen). Cellular attachment experiments were performed using murine astrocyte cells with passage numbers between 5 and 20. The gold and np-Au samples were exposed to air plasma (Harrick Plasma Cleaner) at 10 W for 30 seconds to reactivate surfaces. Samples with five different surface topographies (i.e., Au, untreated np-Au, and np-Au treated at three different

temperatures) were placed in a 24-well culture plate in triplicates. The astrocytes were passaged and seeded onto the samples within a 1 mL of media per well to a final density of 48,000 cells/mL. Cell culture was maintained in a humidified incubator at 37°C with 5% CO_2. After 24 hours, the cells were fixed with 4% paraformaldehyde in phosphate buffered saline (PBS) solution for 20 minutes at room temperature. Following treatment with 0.1% TritonX-100 in PBS for 5 minutes to permeabilize cellular membrane, the f-actin cytoskeleton was stained via treatment with a solution of 300 nM phalloidin (conjugated with Alexa 488 fluorophore, Invitrogen) and 1% bovine serum albumin in PBS for 20 minutes at room temperature. The cellular nuclei were counter-stained with 3 nM DAPI in PBS for 5 minutes. The samples were mounted onto glass slides for imaging with an epifluorescent microscope (Zeiss Axiovert). A total of ten images (845 μm by 670 μm) were captured at arbitrary locations over the metal spots for each sample type. ImageJ software with a custom macro was used to extract the number of cells in each image (from DAPI images) and *average cell area* (from f-actin images). *Cell density* was calculated for each surface via dividing the number of cells in an image by the image area. A set of samples were prepared to be imaged with SEM for visualizing the cellular attachment to surfaces with different topography at an ultra-structural level. Briefly, the cells were fixed with 2.5% glutaraldehyde in PBS for 20 minutes at room temperature and dehydrated in graded ethanol solutions (20%, 50%, 75%, 90%, 95%, 100%) for 5 minutes in each concentration. Finally, the cells were immersed in hexamethyldisilazane (Sigma) to complete drying while minimizing capillary forces that lead to deformation of cellular features. The cells were coated with a thin layer of gold and imaged with the SEM. Single-variable ANOVA available in Excel statistical analysis toolkit (Microsoft Corporation) was used for comparing the cell attachment results between different sample surfaces. A p-value less than 0.05 was deemed statistically significant.

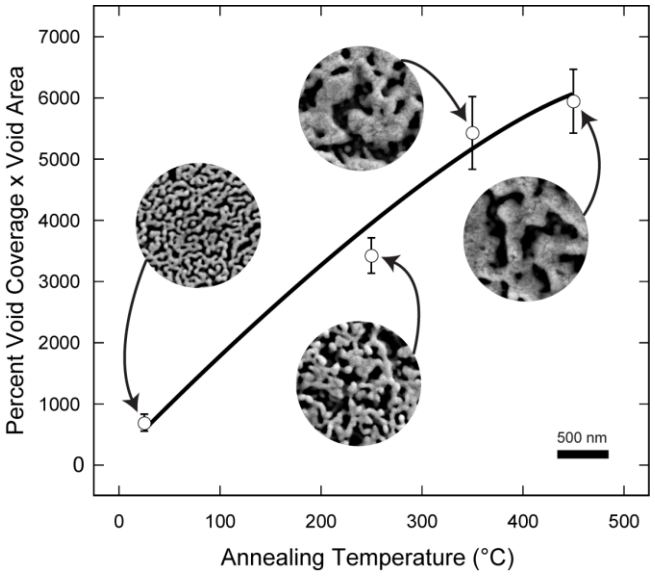

Figure 1. Scanning electron microscope images of the nanoporous gold surfaces obtained by treatment at different temperatures illustrate that the product of percent void coverage and void area increases with treatment temperature. Note that the image corresponding to 25°C illustrates "no thermal treatment" condition. The error bars display standard deviations in measurements and trendlines are visual guides.

III. Results and Discussion

A. Thermal Treatment and Surface Morphology

In order for novel materials to be truly useful, they need to be compatible with conventional microfabrication processes for integration with micro-systems. Since gold-silver alloys (precursor to np-Au) can be deposited and micropatterned with common microfabrication techniques, np-Au can be readily integrated with electronics, greatly expanding its utility in miniaturized biomedical devices, for example, in neural interfaces [4, 7]. During the synthesis of np-Au, silver atoms are stripped by the strong acid and gold atoms diffuse at the metal-electrolyte interface to self-assemble a porous structure [8], shown in Fig. 1 and Fig. 2. Following the dissolution process, residual silver encapsulated within the gold ligaments is typically 2-3% (atomic %). The SEM examination of the engineered surfaces in SE-detector mode provided sufficient image contrast to infer topographical information, which reveal comparable results to AFM studies of np-Au surfaces [17]. Before thermal treatment for coarsening nanotopography, np-Au gold films typically had a percent void coverage of 24.6±1.6 and an average void area of 2800±500 nm^2, as determined by image processing. Thermal treatment led to a maximum percent void coverage of 32.5±0.8 and an average void area of 23700±2000 nm^2. Thermal treatment of the porous structure leads to pore coarsening while not significantly altering the percent coverage by surface voids. The percent void coverage had a non-monotonic dependence on thermal treatment. In order to take into account the changes in both parameters (i.e., percent void coverage and void area) we established their product as a *nanotopography index*. Fig. 1 illustrates that the nanotopography index increases with thermal treatment temperature, offering a range of nanotopographies to evaluate the corresponding cellular response.

B. Cellular Attachment on Different Surfaces

Nanotopography has an effect on multiple aspects of cellular behavior, including differentiation, growth, and viability [18, 19]. We focused on the effect of nanotopography on cell density (surrogate for cell viability)

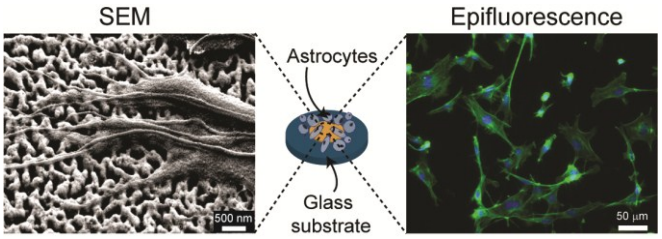

Figure 2. The schematic summarizes the experiment, where astrocystes are cultured on gold spots with varying nanotopography (middle). The cells are stained in green and blue to visualize cytoskeleton and nuclei respectively (right). SEM samples were prepared for qualitative observation of the interaction between cellular processes and nanostructure (left).

and average cell area (surrogate for cell adhesion strength). The rationale for choosing these two parameters is that: (i) non-viable astrocytes detach from the surface and adherent cell density in comparison to biocompatible surfaces (e.g., planar gold [20]) is a measure of a surface's biocompatibility; and (ii) cells make focal adhesions to the underlying surface and a stronger adhesion generally manifests itself by increased cell spreading, as the cell can consequently withstand larger in-plane tensile stresses [21]. Fig. 2 displays an epifluorescent image of cells cultured on np-Au, as well as a SEM image. The SEM image shows that the fine cellular processes conform to the nanotopography. It is possible that physical latching onto surface voids may constitute a complementary attachment mechanism to ligand-based focal adhesions to the surface. Further studies are underway to elucidate this hypothesis. Overall, there was no statistical difference between cell density on different surfaces (ANOVA p-value=0.19, n=50), as shown in Fig. 3 and Fig. 4. As a first approximation, the cell density is a good marker of cell viability. Gold is generally accepted as a biocompatible material [20]. However, a significant number of studies have indicated that biocompatibility can vary significantly as a result of biophysicochemical material-cell interactions at the nano-scale [22]. We therefore initially tested whether np-Au affects cell viability by quantifying the population density of cells attached on each surface. The statistically-indifferent cell densities on surfaces with varying nanotopographies suggest that none of the surfaces had an adverse effect on cell viability. The average area for adherent cells on different surfaces, however, was affected by the nanotopography as shown in Fig. 3 and Fig. 4 (ANOVA p-value=10^{-23}, n=50). Specifically, the average cell area decreased monotonically with increasing percent void coverage (Fig. 3). It is probable that surfaces with higher percent void coverage decreased the available sites for cells to form focal adhesions, thereby reducing average cell area [23].

On the other hand, while average cell area was lower for

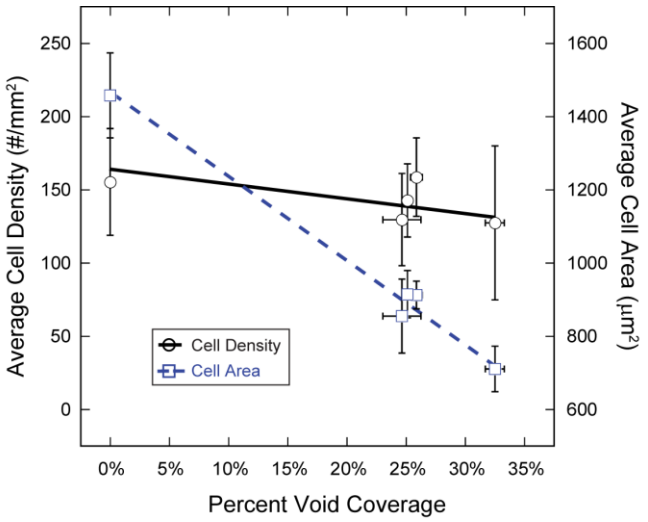

Figure 3. Cell density does not exhibit a statistically-different dependence on percent void coverage. Average cell area is inversely proportional to percent void coverage. The error bars display standard deviations in measurements and trendlines are visual guides.

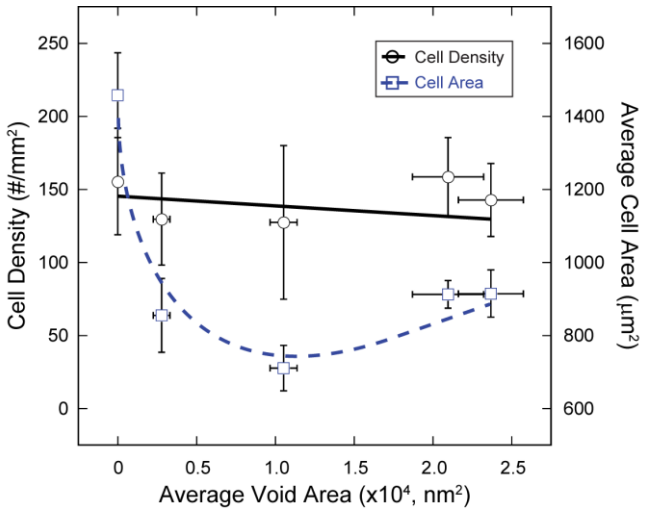

Figure 4. Cell density does not exhibit a statistically-different dependence on average void area. Average cell area displays a non-monotonic decrease with respect to increasing void area. The error bars display standard deviations in measurements and trendlines are visual guides.

cells cultured on np-Au compared to the planar gold surfaces, cell area exhibited a non-monotonic dependence on average void area, as shown in Fig. 4. Relatively large standard deviations in cell density and average cell area are attributed to innate variability of cell proliferation. Overall, as the nanotopography index increased, the average cell area exhibited a similar dependence to that in Fig. 4. This is an expected result, since thermal treatment led to much larger variations (order of magnitude change) in average void area compared to percent void coverage. Even though we cannot completely explain the underlying reasons for the non-monotonic dependence, this observation poses the question of whether different cell types favor a specific nanotopography compatible with their particular cellular architecture (e.g., distribution focal adhesions, cytoskeletal structure [24]) that maximizes adhesion strength. In order to fully test this hypothesis, it is necessary to evaluate a range of topographies that span nano- to micro-scale patterns and quantify focal adhesion densities along with different cell types. Np-Au has a tunable pore range within tens of nanometers to more than 500 nm void diameter. As np-Au can be deposited by conventional microfabrication techniques, supporting substrates can be micropatterned to contain surfaces with topography in the micrometer range. The combination of the two fabrication schemes would create surfaces with a wide range of topographies that can allow for testing the "cell-specific adhesion" hypothesis and designing custom surfaces that promote the attachment of different cell types.

IV. Conclusion

We demonstrated that nanoporous gold is permissive to adherent cell culture at varying degrees of nanotopography without a significant effect on cell density. However, nanotopography had a significant effect on average cell area. The dependence of average cell area to nanotopography is non-monotonic, which suggests that the topography can be tuned to modulate cellular adhesion. Our current focus is on

studying the differences between cell types in their adhesion behavior to a collection of topographies ranging from nano- to micro-scale. We expect this study to benefit biomedical device coatings.

REFERENCES

[1] M.C. Roco, "Nanotechnology: convergence with modern biology and medicine," *Curr. Opin. Biotechnol.*, vol. 14, (no. 3), pp. 337-346, 2003.

[2] I.Y. Wong, B.D. Almquist, and N.A. Melosh, "Dynamic actuation using nano-bio interfaces," *Mater. Today*, vol. 13, (no. 6), pp. 14-22, 2010.

[3] C.E. Ashley, E.C. Carnes, G.K. Phillips, D. Padilla, P.N. Durfee, P.A. Brown, T.N. Hanna, J. Liu, B. Phillips, and M.B. Carter, "The targeted delivery of multicomponent cargos to cancer cells by nanoporous particle-supported lipid bilayers," *Nature Materials*, vol. 10, (no. 5), pp. 389-397, 2011.

[4] N. Kotov, J. Winter, I. Clements, E. Jan, B. Timko, S. Campidelli, S. Pathak, A. Mazzatenta, C. Lieber, and M. Prato, "Nanomaterials for Neural Interfaces," *Adv. Mater.*, vol. 21, (no. 40), pp. 3970-4004, 2009.

[5] E. Gultepe, D. Nagesha, S. Sridhar, and M. Amiji, "Nanoporous inorganic membranes or coatings for sustained drug delivery in implantable devices," *Advanced drug delivery reviews*, vol. 62, (no. 3), pp. 305-315, 2010.

[6] M.M. Stevens and J.H. George, "Exploring and engineering the cell surface interface," *Science*, vol. 310, (no. 5751), pp. 1135, 2005.

[7] D. Hoffman-Kim, J.A. Mitchel, and R.V. Bellamkonda, "Topography, cell response, and nerve regeneration," *Annual review of biomedical engineering*, vol. 12, pp. 203, 2010.

[8] J. Erlebacher, M. Aziz, A. Karma, N. Dimitrov, and K. Sieradzki, "Evolution of nanoporosity in dealloying," *Nature*, vol. 410, (no. 6827), pp. 450-453, 2001.

[9] J. Snyder, T. Fujita, M. Chen, and J. Erlebacher, "Oxygen reduction in nanoporous metal–ionic liquid composite electrocatalysts," *Nature Materials*, vol. 9, pp. 904-907, 2010.

[10] J. Weissmüller, R. Newman, H. Jin, A. Hodge, and J. Kysar, "Theme Article - Nanoporous Metals by Alloy Corrosion: Formation and Mechanical Properties," *Materials Research Society Bulletin*, vol. 34, (no. 8), pp. 577-586 2009.

[11] Z. Liu and P. Searson, "Single nanoporous gold nanowire sensors," *J. Phys. Chem. B*, vol. 110, (no. 9), pp. 4318-4322, 2006.

[12] E. Seker, Y. Berdichevsky, M. Begley, M. Reed, K. Staley, and M. Yarmush, "The fabrication of low-impedance nanoporous gold multiple-electrode arrays for neural electrophysiology studies," *Nanotechnology*, vol. 21, pp. 125504, 2010.

[13] D. Fine, A. Grattoni, S. Hosali, A. Ziemys, E. De Rosa, J. Gill, R. Medema, L. Hudson, M. Kojic, and M. Milosevic, "A robust nanofluidic membrane with tunable zero-order release for implantable dose specific drug delivery," *Lab Chip*, vol. 10, (no. 22), pp. 3074-3083, 2010.

[14] E. Seker, Y. Berdichevsky, K.J. Staley, and M.L. Yarmush, "Microfabrication-Compatible Nanoporous Gold Foams as Biomaterials for Drug Delivery," *Advanced Healthcare Materials*, vol. 1, (no. 2), pp. 172–176, 2012.

[15] E. Seker, J. Gaskins, H. Bart-Smith, J. Zhu, M. Reed, G. Zangari, R. Kelly, and M. Begley, "The effects of post-fabrication annealing on the mechanical properties of freestanding nanoporous gold structures," *Acta Mater.*, vol. 55, (no. 14), pp. 4593-4602, 2007.

[16] F. Velasco, "Thresholding using the ISODATA clustering algorithm," *IEEE Transactions on Systems Man and Cybernetics*, vol. 10, pp. 771-774, 1980.

[17] O. Shulga, K. Jefferson, A. Khan, V. D'Souza, J. Liu, A. Demchenko, and K. Stine, "Preparation and characterization of porous gold and its application as a platform for immobilization of acetylcholine esterase," *Chem. Mater.*, vol. 19, (no. 16), pp. 3902, 2007.

[18] L.E. McNamara, R. Burchmore, M.O. Riehle, P. Herzyk, M.J.P. Biggs, C.D.W. Wilkinson, A.S.G. Curtis, and M.J. Dalby, "The role of microtopography in cellular mechanotransduction," *Biomaterials*, vol. 33, (no. 10), pp. 2835–2847, 2012.

[19] C.J. Bettinger, R. Langer, and J.T. Borenstein, "Engineering Substrate Topography at the Micro and Nanoscale to Control Cell Function," *Angew. Chem. Int. Ed.*, vol. 48, (no. 30), pp. 5406-5415, 2009.

[20] G. Voskerician, M.S. Shive, R.S. Shawgo, H. Recum, J.M. Anderson, M.J. Cima, and R. Langer, "Biocompatibility and biofouling of MEMS drug delivery devices," *Biomaterials*, vol. 24, (no. 11), pp. 1959-1967, 2003.

[21] N.D. Gallant, K.E. Michael, and A.J. Garcia, "Cell adhesion strengthening: contributions of adhesive area, integrin binding, and focal adhesion assembly," *Molecular biology of the cell*, vol. 16, (no. 9), pp. 4329-4340, 2005.

[22] A.E. Nel, L. Madler, D. Velegol, T. Xia, E.M.V. Hoek, P. Somasundaran, F. Klaessig, V. Castranova, and M. Thompson, "Understanding biophysicochemical interactions at the nano-bio interface," *Nature Materials*, vol. 8, (no. 7), pp. 543-557, 2009.

[23] P. Decuzzi and M. Ferrari, "Modulating cellular adhesion through nanotopography," *Biomaterials*, vol. 31, (no. 1), pp. 173-179, 2010.

[24] D.E. Ingber, "Cellular tensegrity: defining new rules of biological design that govern the cytoskeleton," *J. Cell Sci.*, vol. 104, pp. 613-613, 1993.